HHS Public Access

Author manuscript

Nat Chem Biol. Author manuscript; available in PMC 2011 July 01.

Published in final edited form as:

Nat Chem Biol. 2011 January ; 7(1): 34–40. doi:10.1038/nchembio.478.

Signaling Diversity of PKA Achieved Via a Ca^{2+}-cAMP-PKA Oscillatory Circuit

Qiang Ni[1,*], **Ambhighainath Ganesan**[2,*], **Nwe-Nwe Aye-Han**[1,*], **Xinxin Gao**[1], **Michael D. Allen**[1], **Andre Levchenko**[2], and **Jin Zhang**[1,3]

[1] Department of Pharmacology and Molecular Sciences, The Johns Hopkins University School of Medicine, Baltimore, MD 21205

[2] Department of Biomedical Engineering, The Johns Hopkins University School of Medicine, Baltimore, MD 21205

[3] The Solomon H. Snyder Department of Neuroscience and Department of Oncology, The Johns Hopkins University School of Medicine, Baltimore, MD 21205

Abstract

Many protein kinases are key nodal signaling molecules that regulate a wide range of cellular functions. These functions may require complex spatiotemporal regulation of kinase activities. Here, we show that Protein Kinase A (PKA), Ca^{2+} and cAMP oscillate in sync in insulin-secreting MIN6 β cells, forming a highly integrated oscillatory circuit. We found that PKA activity was essential for this oscillatory circuit, and was capable of not only initiating the signaling oscillations but also modulating their frequency, thereby diversifying the spatiotemporal control of downstream signaling. Our findings suggest that exquisite temporal control of kinase activity, mediated via signaling circuits resulting from cross-regulation of signaling pathways, can encode diverse inputs into temporal parameters such as oscillation frequency, which in turn contributes to proper regulation of complex cellular functions in a context-dependent manner.

Protein kinases serve as major information transducers in cells and are responsible for regulating diverse cellular functions1,2. However, the molecular mechanisms underlying this signaling diversity are not well understood, particularly with regard to the role of the spatiotemporal regulation of kinases. Although important progress has been made in increasing our understanding of the spatial compartmentation of kinases3,4, much less is

To whom correspondence should be addressed: Jin Zhang, 725 North Wolfe Street, Hunterian #307, Baltimore, MD 21205. jzhang32@jhmi.edu; Andre Levchenko, 3400 N. Charles St., 208C Clark Hall, Baltimore, MD 21218. alev@jhu.edu.

*These authors contributed equally to this work

Author Contributions

Q.N. and J. Z. conceived the experimental aspect of the project and did the initial experiments; A. L. designed the modeling aspect of the project. Q.N. and N.A. performed the majority of the experiments. A.G. constructed the mathematic model and performed the simulations. G. X. performed the western analyses. M.D.A. designed and generated one of the biosensors. J. Z., Q. N. and A.L. wrote the manuscript.

Competing Financial Interests

The authors declare no competing financial interests.

known about how temporal regulation of kinase action can be exploited to encode diverse signals and control different functional outcomes5.

PKA, a prototypical protein kinase6, plays a host of important roles in diverse cellular locations. Among these is the regulation of Ca^{2+}-triggered exocytosis at the cell membrane, a process critical to many cellular functions7. In pancreatic β cells, exocytosis is critical for the pulsatile insulin secretion that is regulated by a variety of stimuli, including electric, metabolic and hormonal signals8,9. Ca^{2+} influx is stimulated when glucose metabolism produces an increase in the [ATP]/[ADP] ratio that inhibits K-ATP channels and induces membrane depolarization, leading to the opening of voltage-gated Ca^{2+} channels. When activated either by glucose10 via Ca^{2+} or by hormones such as glucagon-like peptide-1 via classical G-protein-coupled receptor signaling9, PKA can in turn modulate the Ca^{2+} signal11,12 and also directly influence exocytotic insulin release7. For instance, a PKA-dependent mechanism operates during the initial phase of glucose-induced excytosis13, and impairment of this process has been implicated in the pathogenesis of type 2 diabetes14.

Here, we investigated the role of the temporal regulation of PKA in integrating and transducing diverse signals. By combining fluorescent biosensor-based live-cell tracking of signaling activities with mechanistic modeling, we demonstrate that PKA exhibits oscillatory activity and, together with Ca^{2+} and cAMP, forms a highly integrated oscillatory circuit in MIN6 β cells. The organization of this oscillatory circuit allows PKA to modulate the frequency of oscillation, to integrate input signals and to exert diverse spatiotemporal controls on substrate phosphorylation. This demonstration of a functional role for the temporal regulation of a protein kinase in achieving signaling diversity helps to establish a new model for encoding signaling information into temporal parameters, such as the frequency of oscillation, of an enzymatic activity.

Results

Oscillatory PKA activity

We set out to analyze the temporal patterns of PKA activity in MIN6 β cells treated with tetraethylammonium chloride (TEA), a pharmacological agent that induces membrane depolarization to trigger a Ca^{2+} signal15. Under this condition, both Ca^{2+} and cAMP have been shown to undergo oscillations16. It is therefore interesting to examine the activity pattern of PKA in this context because PKA activity may exhibit a range of dynamic behaviors depending on the relationship between the dynamics of the cAMP oscillatory input and PKA activation/inactivation kinetics. As illustrated in Figure 1A (See Section VIIIA of Supplementary Methods for details), PKA activity could exhibit monotonic increases when the input oscillation frequency is much greater than the rates of the PKA activation/inactivation kinetics (top panel, Figure 1A), oscillatory changes when these values match (bottom panel, Figure 1A), or semi-oscillatory intermediate responses (middle panel, Figure 1A).

We first analyzed PKA activity at the cell population level17,18, using an antibody against the phosphorylated consensus substrate motif of PKA. Sustained monotonic increases in substrate phosphorylation by PKA were observed in MIN6 cells treated with TEA

(Supplementary Figure 1), suggesting that PKA activity might not conform to cAMP oscillations or that the oscillatory PKA activity is masked at the cell-population level. To analyze the temporal dynamics of PKA at the single-cell level, we performed fluorescence imaging of endogenous PKA activity using a genetically encoded A-kinase activity reporter (AKAR)19,20. In contrast to the population results, this analysis revealed oscillatory PKA activity (Figure 1B and 1C), suggesting a repetitive shifting of the balance between the actions of PKA and counteracting phosphatases in single cells. These oscillations occurred with a period of 1–6 min in >60% of AKAR-expressing MIN6 cells (n = 21), matching the frequency of the Ca^{2+} oscillation patterns previously reported in these cells16. Therefore, PKA activity exhibits oscillatory changes in single MIN6 cells, which were likely masked in cell population studies because the observed oscillations in PKA activities were asynchronous, varying in phase and frequency among individual cells.

Synchronized oscillations of PKA, Ca^{2+} and cAMP

Given that Ca^{2+} is known to oscillate under the same conditions and to serve as an important signal in β cells, we characterized the temporal correlation between PKA activity and Ca^{2+} dynamics by performing co-imaging experiments using AKAR in conjunction with the Ca^{2+} dye Fura-221 in single MIN6 cells. For these experiments, we engineered a red-shifted AKAR, AKAR-GR (Figure 2A and Supplementary Figure 2A) based on EGFP, and the red fluorescent protein mCherry, to allow better signal separation from Fura-2. We found that the PKA oscillations and Ca^{2+} oscillations were “in register” with each other (Figure 2B). Notably, during each cycle of oscillation, the rise in the Ca^{2+} transient appeared to follow, with a noticeable lag, the accumulation of PKA activity (Figure 2B). This pattern likely reflected the PKA-mediated potentiation of Ca^{2+} influx via voltage-gated Ca^{2+} channels and/or inositol trisphosphate receptors (IP_3R)22,23. Moreover, the decrease in PKA activity in each cycle was surprisingly rapid when compared to the transient PKA activities observed in other cell types (Supplementary Figure 3)24, and it was precisely correlated with the Ca^{2+} spike, suggesting that there is a Ca^{2+}-dependent mechanism in place to ensure the rapid down-regulation of and/or counterbalancing of PKA activity.

In MIN6 cells, Ca^{2+}-dependent regulation of PKA can occur through Ca^{2+} dependent adenylate cyclases (ACs) and phosphodiesterases (PDEs)7, the enzymes that produce and degrade cAMP, respectively. Indeed, as previously observed,16 cAMP was found to oscillate under the same conditions when visualized with a fluorescent cAMP indicator, ICUE25,26 (Supplementary Figure 4). Simultaneous imaging using a red-shifted ICUE, ICUE-YR (Figure 2A, and Supplementary Figure 2B), and Fura-2 in single MIN6 cells confirmed that these cAMP oscillations are highly synchronized with the Ca^{2+} oscillations (Figure 2C).

The high degree of synchronization between PKA and Ca^{2+} and between cAMP and Ca^{2+} suggested that all three components were regulated in a temporally coordinated fashion. Since PKA activity is often compartmentalized in various systems3, we asked if the cAMP and PKA oscillations were also correlated in the local cellular context. To answer this question, we took advantage of a new single-chain dual-specificity biosensor for parallel detection of PKA activity and cAMP dynamics (Figure 2A, and Supplementary Figure 5).

This biosensor contains both cAMP-sensitive and PKA-dependent molecular switches and can simultaneously capture the dynamics of two signaling events in the same local environment, thereby facilitating quantification and correlation of these signaling activities. In MIN6 cells expressing this single-chain dual-specificity biosensor, TEA treatment elicited oscillatory signals from both reporting units (Figure 2D). These oscillations were highly temporally coordinated, with cAMP rises always preceding increases in PKA activity (Figure 2D), suggesting that oscillations in PKA activities are indeed locally driven by oscillatory changes in cAMP levels.

Analysis of the Ca^{2+}-cAMP-PKA oscillatory circuit

The precise temporal correlation between the oscillatory activities of Ca^{2+}, cAMP and PKA suggests a complex underlying mechanism involving multiple feedback interactions. To better understand this signaling circuit, we constructed a mathematical model by incorporating a detailed description of the biochemical events involving these three key molecular components. In our model (described in detail in the Supplementary Methods), the interplay between the membrane-potential regulation and $[Ca^{2+}]$ forms the first feedback loop, consistent with the Chay-Keizer model27. A second feedback loop, centered around Ca^{2+}, cAMP and PKA, was incorporated by explicitly introducing putative regulation of both voltage-gated L-type Ca^{2+} channels and IP_3R by active PKA22,23. Additional links needed to complete the model were introduced on the basis of a network topology analysis determining the minimal model sufficient to account for several qualitative features of our experimental findings (see Supplementary Methods Section III for complete model description and analysis). When operating under assumptions about parameter values consistent with literature data, the model was able to capture the detailed dynamic relationships between various molecular components observed in our experiments (Figure 2E-G). Our combined experimental and modeling data therefore suggested the existence of a functional signaling circuit consisting of Ca^{2+}, cAMP and PKA. In this circuit, the activities of all the components are temporally regulated in the form of synchronized oscillations, as a result of a tight coupling between these components through feedback interactions.

Role of PKA in the oscillatory circuit

To dissect the role of PKA in this oscillatory circuit, we examined the effects of altered PKA activity on the oscillatory patterns of the Ca^{2+}-cAMP-PKA system. The model predicted that the oscillatory behavior of the system, as indicated by the Ca^{2+} signal, would strongly depend on the level of PKA activity, although oscillation of PKA activity was not required for maintaining Ca^{2+} oscillations (Supplementary Figure 6). As shown in Figure 3A, inhibition of PKA activity was predicted to have strong abolishing effects on Ca^{2+} oscillations. Indeed, addition of the PKA inhibitor H89 to MIN6 cells rapidly terminated Ca^{2+} oscillations, indicating that PKA activity was required (Figure 3B and Supplementary Figure 7A). Consistent with this observation, no TEA-induced Ca^{2+} oscillations were observed in 17 of 24 cells in the presence of a specific PKA inhibitor, mCherry-tagged PKI. This result represents a 3-fold reduction in oscillatory behavior compared to control cells, over 87% of which showed Ca^{2+} oscillations (Supplementary Figure 7C). In contrast, the model predicted that increasing PKA activity would modulate the frequency of the Ca^{2+} oscillations (Figure 3C). This prediction was tested by monitoring Ca^{2+} dynamics when a

general phosphodiesterase inhibitor, 3-isobutyl-1-methylxanthine (IBMX), was added to MIN6 cells after TEA-induced Ca^{2+} oscillations were established. We found that every cell showing regular oscillations both before and after IBMX addition exhibited an increase in oscillation frequency (n = 15) (Figure 3D and Supplementary Figure 7B), demonstrating that cAMP/PKA activity can modulate the Ca^{2+} oscillation frequency.

On the other hand, PKA-mediated phosphorylation is continuously counterbalanced by phosphatase activity. For instance, PKA and phosphatase PP2B are known to have opposing effects on L-type Ca^{2+} channels via phosphorylation and dephosphorylation of the channels, respectively28. Our model predicted that changes in PP2B activity would have an effect opposite to that of PKA activity in terms of modulating the frequency of Ca^{2+} oscillations (Figure 3E). Consistent with this prediction, treatment of MIN6 cells with 3 μM cyclosporine A, a PP2B inhibitor, increased the frequency of TEA-induced Ca^{2+} oscillations (n = 7) (Figure 3F), indicating that the ability of PKA to modulate Ca^{2+} oscillation is under the influence of opposing phosphatase activities.

Interestingly, model simulations also showed that when compared to the Ca^{2+} oscillation amplitude, the oscillation frequency was considerably more sensitive to changes in PKA activity and variation of other model parameters (Figure 3G, 3H and Supplementary Figures 8–12). This finding suggests a role for PKA as a frequency modulator. Taken together, these data suggest that PKA activity can directly modulate the oscillatory patterns of the Ca^{2+}-cAMP-PKA signaling circuit, thereby affecting cellular processes under the control of Ca^{2+}.

Direct activation of PKA triggers the oscillatory circuit

β cells are constantly subject to regulation by a broad range of distinct signals, including electric, metabolic and hormonal signals8,9. Given the tunability of this signaling circuit and the capacity of its major components to connect to different signal-sensing networks29,30, one of its important functions may be to integrate multiple input signals that can independently activate the circuit's components. Thus, it is possible that various signals, via direct activation of different components, can trigger the oscillations of this signaling system. To test this hypothesis, 1–3 μM of 8-bromoadenosine-3′,5′-cyclic monophosphate-acetoxymethylester, a cAMP analog that preferentially activates PKA, was added to MIN6 cells expressing AKAR. In over 40% of the cells (n = 16), the addition of this cAMP analog alone triggered oscillatory changes in PKA activity (Figure 4A and Supplementary Figure 13), similar to the TEA-induced oscillations. Furthermore, different strengths of the input signals could apparently be encoded into different activity patterns, because higher doses (10–20 μM) of the same cAMP analog triggered a gradual increase in PKA activity with a small-amplitude higher-frequency oscillatory change superimposed on the monotonic activation rise (Figure 4A) (n = 13). Our mathematical model captured the basic characteristics of the oscillations induced by direct activation of PKA (Figure 4B) and suggested that sufficiently strong PKA feedback can initiate oscillations even when the feedback loop involving Ca^{2+} and membrane potential is initially inactive. Furthermore, the distinct PKA activity patterns induced by low doses and high doses of cAMP (Figure 4) showed an elaborate transition of behaviors that is indicative of the frequency change of the oscillatory circuit. Thus, PKA is an integral component of the oscillatory circuit and is

capable of not only tuning but also enabling the oscillatory circuit behaviors in response to specific input signals.

Spatiotemporal controls via oscillatory PKA activity

Each of the key components of the oscillatory circuit — Ca^{2+}, cAMP and PKA, regulates a diverse set of cellular functions with high specificity. In the case of PKA, spatial compartmentation of PKA-dependent signaling has been identified as an important mechanism underlying specific regulation of distinct functions3. We propose that the oscillatory PKA activity enabled by the Ca^{2+}-cAMP-PKA circuit can serve as a distinct mechanism for achieving signaling diversity.

At the level of temporal regulation, given an oscillatory PKA activity, both oscillatory and sustained phosphorylation of PKA substrates can be achieved, depending on the access of the substrate to phosphatases reversing PKA phosphorylation (Supplementary Figure 14). For example, recruitment of PKA and phosphatase PP2B to L-type Ca^{2+} channels can ensure efficient and rapid phosphorylation and dephosphorylation within this signaling complex28. Repetitive phosphorylation of the channels, which has been suggested in previous studies to be critical for proper β cell function31, would in turn ensure that the activity of the channel reaches certain threshold level only periodically; this pattern would decrease the probability of spontaneous channel openings between insulin secretion phases. In contrast, PKA targets devoid of high local phosphatase activity can integrate multiple oscillation phases over time, thus enabling a distinct mode of regulation.

More exquisite spatial control of PKA activity may also be achieved via oscillations. For instance, cAMP/PKA signaling microdomains, such as those defined by AKAP-assembled signaling complexes, may also depend on the kinetics of signaling reactions and the presence of regulatory feedback interactions32. A local PKA signaling complex is typically assembled by A-Kinase anchoring protein (AKAP) binding to the regulatory (R) but not the catalytic (C) subunit of PKA. This signaling compartmentalization can be lost if the unanchored C-subunit diffuses away after dissociation from the R subunit, rather than being recaptured when cAMP dissociates from the R subunits. It is thus paradoxical that local PKA activity can be maintained for prolonged periods of time. Our model suggests that, under the experimental conditions analyzed above, this apparent paradox can be resolved, since the oscillatory circuit is capable of maintaining a relatively low time-averaged PKA activity, while having relatively high maximal peak PKA activity (Figure 5A; local activation regime). The low average PKA activity implies a low average free concentration of the C-subunit in the signaling domain and thus a low escape rate of the subunit from the domain. Recapture of the C-subunit can help reset the local PKA activity cycle. At the same time, the peak PKA activity can periodically exceed the threshold levels needed for full activation of the target substrates and would be further enhanced if the substrates have limited access to the corresponding phosphatases (Figure 5A). On the other hand, an enhanced input into PKA activation and the resulting high average PKA activity could lead to increased escape of the C subunit from a local signaling domain (Figure 5A; global activation regime). At the subcellular organelle level, increased escape of the C-subunit from a cytosolic signaling compartment could result in the C-subunit's translocation into the

nucleus (Supplementary Figure 15). We sought to experimentally validate this prediction. Indeed, we found that while low doses of a cAMP analog induced oscillations in the cytosol without affecting nuclear PKA activity or phosphorylation of an endogenous transcription factor CREB, the gradual increase in PKA activity with superimposed high-frequency oscillation induced by high doses of the analog led to an increase in nuclear PKA activity and CREB phosphorylation (Figure 5B - D and Supplementary Figure 16). This effect on CREB phosphorylation was also observed with the co-treatment of CsA or IBMX with a low dose of the cAMP analog (Supplementary Figure 17) or with TEA (Supplementary Figure 18). Thus, the oscillatory PKA activity can apparently encode context-dependent spatiotemporal information for controlling diverse output signals.

Discussion

Oscillation of signaling activity can be a versatile mechanism for achieving diversity and specificity. This notion was first demonstrated in the case of Ca^{2+} oscillation, the frequencies of which are determined by the amount and type of extracellular signals33–35 and can influence the efficiency and specificity of gene expression36,37. Our analysis suggests that, as in the case of Ca^{2+} oscillations, the frequency of PKA activity oscillation can be used as a signaling currency, integrating input signals according to their identities and doses and generating specific functional output (e.g., local vs. global signaling modes). In this way, the oscillatory PKA activity allows PKA to function as a versatile signaling transducer that can exert spatiotemporal controls over a variety of functional outcomes in response to specific signals. Future studies will directly evaluate the effects of changing the PKA oscillation frequency on cellular processes that are important to β-cell functions, such as gene expression and insulin secretion.

Our analysis demonstrates that, in addition to transducing signals via activity oscillation, PKA in insulin-secreting cells also plays an active role in shaping the oscillatory patterns of other key components in the signaling circuit, such as Ca^{2+}. This finding is in contrast to previous studies in which oscillations of several protein kinases (e.g., PKA38, PKC39, mitogen-activated protein kinases18,40, and calmodulin-dependent protein kinase II41) were demonstrated, but the potential role of these kinases in shaping the oscillation patterns was not explored. It remains to be seen whether some of these kinases or other candidate kinases are also focal points of oscillatory activities.

Given that each of the key components in the Ca^{2+}-cAMP-PKA circuit can regulate distinct functions, the synchronized oscillations ensure the coordinated activity of these key players, providing a mechanism for achieving efficient and specific control of cellular processes. Therefore, it is reasonable to suggest that complex cellular behaviors may critically depend on such synchronization and coordination of various signaling molecules.

In summary, this current study provides a clear example of exquisite temporal control of a protein kinase within an oscillatory circuit. This signaling system could serve as a paradigm for understanding the spatiotemporal regulation of other signaling networks that control complex cellular processes. Furthermore, given the ubiquitous presence of the key

components of the oscillatory Ca^{2+}-cAMP-PKA circuit42,43, its effects are likely to be widespread, serving to regulate diverse processes in various cell types.

Methods

Gene Construction

EGFP and mCherry were PCR amplified to introduce appropriate restriction digest sites for subcloning into either AKAR or ICUE constructs. The genes of GR-AKAR and YR-ICUE were generated in pRSETB (Invitrogen) and then moved to pcDNA3 (Invitrogen) behind a Kozak sequence for mammalian expression. ICUEPID was generated from CRY-AKAR44 in pcDNA3 by replacing mVenus with the molecular switch and mCitrine of ICUE2.

Cell Culture

MIN6 cells were plated onto sterilized glass coverslips in 35-mm dishes and grown to 50–90% confluency in DMEM (10% FBS) at 37°C with 5% CO_2. Cells were transfected using Lipofactamine 2000 (Invitrogen) and grown 20–48 h before imaging. For Ca^{2+} imaging experiments, cells were preincubated with 1 μM Fura-2/AM (Molecular Probes) for 10–20 min at 37 °C before imaging

Imaging

Cells were washed twice with Hanks' balanced salt solution buffer and maintained in the dark at room temperature. Cells were imaged on a Zeiss Axiovert 200M microscope with a cooled charge-coupled device camera (MicroMAX BFT512, Roper Scientific, Trenton, NJ) controlled by METAFLUOR 6.2 software (Universal Imaging, Downingtown, PA). Fura-2 dual excitation ratio imaging used two excitation filters [350DF10 for 350 nm excitation and 380DF10 for 380 nm excitation], a 450DRLP dichroic mirror, and a 535DF45 emission filter. Dual red/green emission ratio imaging used a 480DF30 excitation filter, a 505DRLP dichroic mirror, and two emission filters [535DF45 for GFP and 653DF95 for RFP]. Dual red/cyan emission ratio imaging used a 420DF20 excitation filter, a 450DRLP dichroic mirror, and two emission filters [475DF40 for CFP and 653DF95 for RFP]. Dual yellow/red emission ratio imaging used a 495DF10 excitation filter, a 515DRLP dichroic mirror, and two emission filters [535DF25 for YFP and 653DF95 for RFP]. Dual cyan/yellow emission ratio imaging used a 420DF20 excitation filter, a 450DRLP dichroic mirror, and two emission filters [475DF40 for CFP and 535DF25 for YFP]. These filters were alternated by a filter-changer Lambda 10–2(Sutter Instruments, Novato, CA). Exposure time was 50–500 ms, and images were taken every 10–30 s. Fluorescence images were background-corrected by subtracting the fluorescence intensity of background with no cells from the emission intensities of cells expressing fluorescent reporters. The ratios of 350/380, red/green, red/cyan, yellow/red, or yellow/cyan emissions were then calculated at different time points. The values of all time courses were normalized by dividing each by the average basal value before drug addition.

Modeling

Simulations were carried out with custom written MATLAB programs. The system has 6 states: membrane potential (V), gating probability of K^+ channel (w), concentration of

cytosolic Ca^{2+} ($[Ca^{2+}]_i$), [cAMP], concentration of cAMP bound regulatory subunits of PKA ($[c_4R_2]$), concentration of free catalytic subunit which is the active PKA ($[PKA^*]$). Kinetic equations for Ca^{2+} flux through the plasma membrane were based on the Chay-Keizer model and the Ca^{2+} release from internal stores was modeled as arising out of the coordinated activities of IP_3Rs and SERCAs. Both the fluxes were dependent on PKA activity, thereby setting up a feedback loop. The increase in $[Ca^{2+}]_i$ modulates the activities of Ca^{2+} inhibitable AC VI and Ca^{2+} activated PDE1, which in turn produce and degrade cAMP respectively. PKA is activated by the sequential binding of 4 molecules of cAMP and the catalytic subunit is released sequentially. Concentrations were normalized with respect to their respective maximal levels, for the ease of comparison. The programs were simulated for a sufficient time span (1000 s for traces and 3000 s for parameter tuning analysis) to produce sustained oscillatory patterns. Frequency of Ca^{2+} oscillations was calculated using MATLAB's in-built FFT routine. A detailed description of the model and the derivation of the ODEs are given in the Supplementary Methods.

Western Analysis

For analysis of oscillatory changes in PKA activity, MIN6 cells were stimulated with 20 mM TEA and washed with ice-cold phosphate-buffered saline at different time points (0, 1, 2, 3, 4, 5, 6, 7, 8 min). Cells were rapidly lysed in radioimmunoprecipitation assay lysis buffer containing protease inhibitor cocktail, 1 mM ethylenediaminetetraacetic acid (EDTA), 1 mM phenylmethylsulfonyl fluoride(PMSF), 1 mM $NaVO_4$, 1 mM NaF, and 25 nM Calyculin A. Cell lysates were incubated on ice for 30 min and centrifuged at 4°C for 20 min. Total protein was separated with 7.5 % SDS-polyacrylamide gel electrophoresis (PAGE) and transferred to nitrocellulose membranes, which were probed with phospho-PKA substrate or β-tubulin antibody. Bands were visualized by enhanced chemiluminescence. The intensity of the bands was quantified, and the values were then normalized to β-tubulin level by using UN-SCAN-IT (Silk Scientific, Orem, UT). For detection of nuclear PKA activity, MIN6 cells were stimulated with low dose (2 μM) or high dose (10 μM) of cAMP analog, or 50 μM forskolin (FSK) and washed with ice-cold phosphate-buffered saline after 45 min incubation. Cells were then lysed as described above. Total protein was separated with 7.5 % SDS-PAGE and transferred to nitrocellulose membranes, then probed with phospho-CREB (pS133) or CREB antibody. The intensity of the bands was quantified. The values of phospho-CREB level then were normalized to CREB expression level.

Supplementary Material

Refer to Web version on PubMed Central for supplementary material.

Acknowledgments

We thank Drs. Jun-Ichi Miyazaki, George G. Holz and Gerald H. Hart for providing cell lines. We also thank Xiong Li for initial technical assistance. This work was supported by National Institutes of Health grants R01 DK073368 and DP1OD006419 (to J. Z.); and GM072024 and RR020839 (to A.L.).

References

1. Manning G, Whyte DB, Martinez R, Hunter T, Sudarsanam S. The protein kinase complement of the human genome. Science. 2002; 298:1912–1934. [PubMed: 12471243]
2. Ubersax JA, Ferrell JE Jr. Mechanisms of specificity in protein phosphorylation. Nat Rev Mol Cell Biol. 2007; 8:530–541. [PubMed: 17585314]
3. Carnegie GK, Means CK, Scott JD. A-kinase anchoring proteins: from protein complexes to physiology and disease. IUBMB Life. 2009; 61:394–406. [PubMed: 19319965]
4. Brown MD, Sacks DB. Protein scaffolds in MAP kinase signalling. Cell Signal. 2009; 21:462–469. [PubMed: 19091303]
5. Marshall CJ. Specificity of receptor tyrosine kinase signaling: transient versus sustained extracellular signal-regulated kinase activation. Cell. 1995; 80:179–185. [PubMed: 7834738]
6. Taylor SS, et al. Signaling through cAMP and cAMP-dependent protein kinase: diverse strategies for drug design. Biochim Biophys Acta. 2008; 1784:16–26. [PubMed: 17996741]
7. Seino S, Shibasaki T. PKA-dependent and PKA-independent pathways for cAMP-regulated exocytosis. Physiol Rev. 2005; 85:1303–1342. [PubMed: 16183914]
8. Bertram R, Sherman A, Satin LS. Metabolic and electrical oscillations: partners in controlling pulsatile insulin secretion. Am J Physiol Endocrinol Metab. 2007; 293:E890–E900. [PubMed: 17666486]
9. Gromada J, Brock B, Schmitz O, Rorsman P. Glucagon-like peptide-1: regulation of insulin secretion and therapeutic potential. Basic Clin Pharmacol Toxicol. 2004; 95:252–262. [PubMed: 15569269]
10. Delmeire D, et al. Type VIII adenylyl cyclase in rat beta cells: coincidence signal detector/ generator for glucose and GLP-1. Diabetologia. 2003; 46:1383–1393. [PubMed: 13680124]
11. Henquin JC, Meissner HP. The ionic, electrical, and secretory effects of endogenous cyclic adenosine monophosphate in mouse pancreatic B cells: studies with forskolin. endo. 1984; 115:1125–1134.
12. Ammala C, Ashcroft FM, Rorsman P. Calcium-independent potentiation of insulin release by cyclic AMP in single beta-cells. Nature. 1993; 363:356–358. [PubMed: 7684514]
13. Hatakeyama H, Kishimoto T, Nemoto T, Kasai H, Takahashi N. Rapid glucose sensing by protein kinase A for insulin exocytosis in mouse pancreatic islets. J Physiol. 2006; 570:271–282. [PubMed: 16284079]
14. Vaag A, Henriksen JE, Madsbad S, Holm N, Beck-Nielsen H. Insulin secretion, insulin action, and hepatic glucose production in identical twins discordant for non-insulin-dependent diabetes mellitus. J Clin Invest. 1995; 95:690–698. [PubMed: 7860750]
15. Ashcroft FM, Rorsman P. Electrophysiology of the pancreatic beta-cell. Prog Biophys Mol Biol. 1989; 54:87–143. [PubMed: 2484976]
16. Landa LR Jr, et al. Interplay of Ca2+ and cAMP signaling in the insulin-secreting MIN6 beta-cell line. J Biol Chem. 2005; 280:31294–31302. [PubMed: 15987680]
17. Maeda M, et al. Periodic signaling controlled by an oscillatory circuit that includes protein kinases ERK2 and PKA. Science. 2004; 304:875–878. [PubMed: 15131307]
18. Hilioti Z, et al. Oscillatory phosphorylation of yeast Fus3 MAP kinase controls periodic gene expression and morphogenesis. Curr Biol. 2008; 18:1700–1706. [PubMed: 18976914]
19. Zhang J, Ma Y, Taylor SS, Tsien RY. Genetically encoded reporters of protein kinase A activity reveal impact of substrate tethering. Proc Natl Acad Sci U S A. 2001; 98:14997–15002. [PubMed: 11752448]
20. Zhang J, Hupfeld CJ, Taylor SS, Olefsky JM, Tsien RY. Insulin disrupts beta-adrenergic signalling to protein kinase A in adipocytes. Nature. 2005; 437:569–573. [PubMed: 16177793]
21. Grynkiewicz G, Poenie M, Tsien RY. A new generation of Ca^{2+} indicators with greatly improved fluorescence properties. J Biol Chem. 1985; 260:3440–3450. [PubMed: 3838314]
22. Leiser M, Fleischer N. cAMP-dependent phosphorylation of the cardiac-type alpha 1 subunit of the voltage-dependent Ca2+ channel in a murine pancreatic beta-cell line. Diabetes. 1996; 45:1412–1418. [PubMed: 8826979]

23. Bugrim AE. Regulation of Ca2+ release by cAMP-dependent protein kinase. A mechanism for agonist-specific calcium signaling? cc. 1999; 25:219–226.
24. Allen MD, Zhang J. Subcellular dynamics of protein kinase A activity visualized by FRET-based reporters. Biochem Biophys Res Commun. 2006; 348:716–721. [PubMed: 16895723]
25. DiPilato LM, Cheng X, Zhang J. Fluorescent indicators of cAMP and Epac activation reveal differential dynamics of cAMP signaling within discrete subcellular compartments. Proc Natl Acad Sci U S A. 2004; 101:16513–16518. [PubMed: 15545605]
26. Violin JD, et al. beta2-adrenergic receptor signaling and desensitization elucidated by quantitative modeling of real time cAMP dynamics. J Biol Chem. 2008; 283:2949–2961. [PubMed: 18045878]
27. Chay TR, Keizer J. Minimal model for membrane oscillations in the pancreatic beta-cell. Biophys J. 1983; 42:181–190. [PubMed: 6305437]
28. Oliveria SF, Dell'Acqua ML, Sather WA. AKAP79/150 anchoring of calcineurin controls neuronal L-type Ca2+ channel activity and nuclear signaling. Neuron. 2007; 55:261–275. [PubMed: 17640527]
29. Bergsten P, Grapengiesser E, Gylfe E, Tengholm A, Hellman B. Synchronous oscillations of cytoplasmic Ca2+ and insulin release in glucose-stimulated pancreatic islets. J Biol Chem. 1994; 269:8749–8753. [PubMed: 8132606]
30. Dyachok O, Isakov Y, Sagetorp J, Tengholm A. Oscillations of cyclic AMP in hormone-stimulated insulin-secreting beta-cells. Nature. 2006; 439:349–352. [PubMed: 16421574]
31. Lester LB, Faux MC, Nauert JB, Scott JD. Targeted protein kinase A and PP-2B regulate insulin secretion through reversible phosphorylation. endo. 2001; 142:1218–1227.
32. Neves SR, et al. Cell shape and negative links in regulatory motifs together control spatial information flow in signaling networks. Cell. 2008; 133:666–680. [PubMed: 18485874]
33. Woods NM, Cuthbertson KSR, Cobbold PH. Repetitive transient rises in cytoplasmic free calcium in hormone-stimulated hepatocytes. Nature. 1986; 319:600–602. [PubMed: 3945348]
34. Berridge MJ, Galione A. Cytosolic calcium oscillators. FASEB J. 1988; 2:3074–3082. [PubMed: 2847949]
35. Putney JW, Bird GS. Cytoplasmic calcium oscillations and store-operated calcium influx. J Physiol. 2008; 586:3055–3059. [PubMed: 18388136]
36. Li W, Llopis J, Whitney M, Zlokarnik G, Tsien RY. Cell-permeant caged $InsP_3$ ester shows that Ca^{2+} spike frequency can optimize gene expression. Nature. 1998; 392:936–941. [PubMed: 9582076]
37. Dolmetsch RE, Xu K, Lewis RS. Calcium oscillations increase the efficacy and specificity of calcium-dependent gene expression. Nature. 1998; 392:933–936. [PubMed: 9582075]
38. Dunn TA, et al. Imaging of cAMP levels and protein kinase A activity reveals that retinal waves drive oscillations in second-messenger cascades. J Neurosci. 2006; 26:12807–12815. [PubMed: 17151284]
39. Violin JD, Zhang J, Tsien RY, Newton AC. A genetically encoded fluorescent reporter reveals oscillatory phosphorylation by protein kinase C. J Cell Biol. 2003; 161:899–909. [PubMed: 12782683]
40. Shankaran H, et al. Rapid and sustained nuclear-cytoplasmic ERK oscillations induced by epidermal growth factor. Mol Syst Biol. 2009; 5:332. [PubMed: 19953086]
41. Markoulaki S, Matson S, Ducibella T. Fertilization stimulates long-lasting oscillations of CaMKII activity in mouse eggs. Dev Biol. 2004; 272:15–25. [PubMed: 15242787]
42. Zaccolo M, Pozzan T. CAMP and Ca2+ interplay: a matter of oscillation patterns. Trends Neurosci. 2003; 26:53–55. [PubMed: 12536124]
43. Borodinsky LN, Spitzer NC. Second messenger pas de deux: the coordinated dance between calcium and cAMP. Sci STKE. 2006; 2006:e22.
44. Allen MD, Zhang J. A tunable FRET circuit for engineering fluorescent biosensors. Angew Chem Int Ed Engl. 2008; 47:500–502. [PubMed: 18058965]

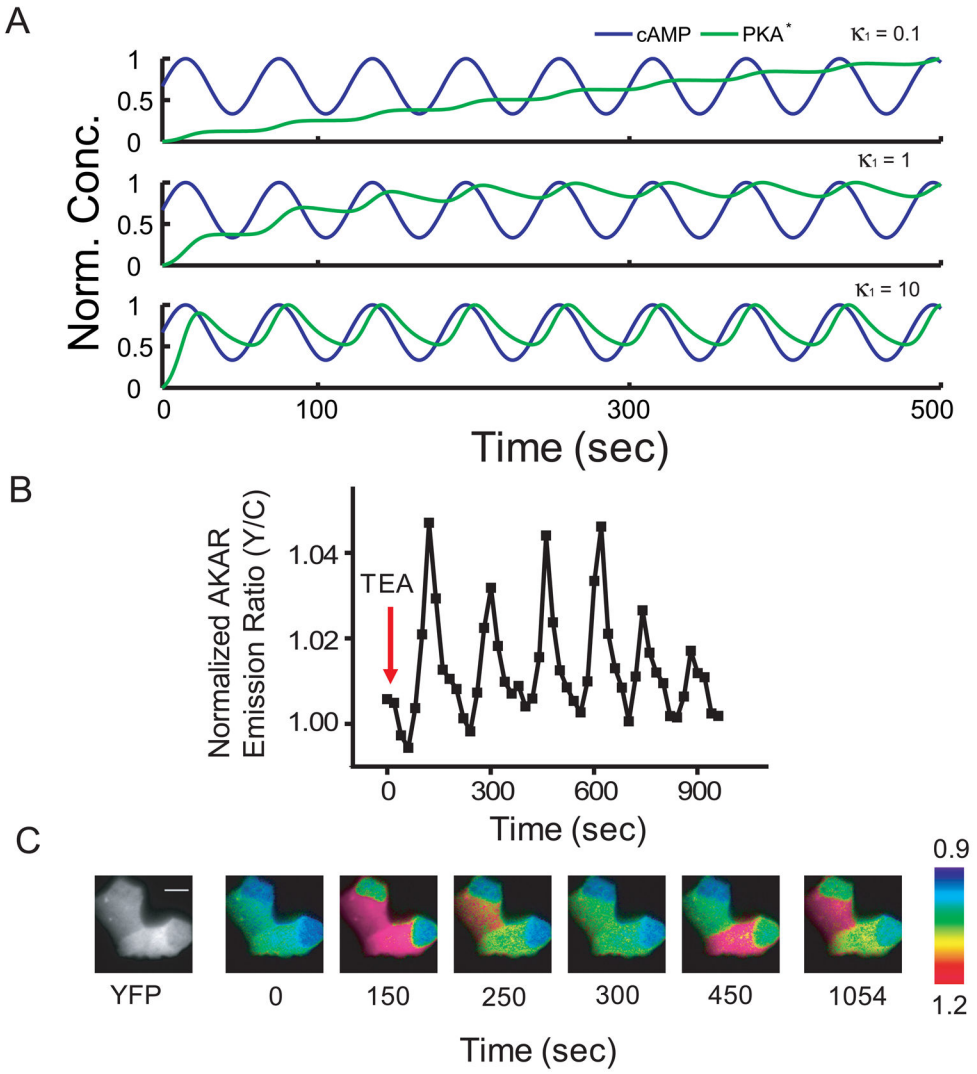

Figure 1.

Oscillatory changes in PKA activity in single MIN6 β cells. (A) Simulation of PKA activity in the presence of oscillatory cAMP, showing different activity patterns depending on the characteristics of the oscillations and parameters of PKA activation and deactivation. The parameter, K_1, reflecting the binding of cAMP to PKA homodimer was varied in this simulation. The parameter κ_1 is the ratio of the new value to the nominal value of K_1. (B) A representative time course of yellow-over-cyan emission ratio changes in single MIN6 β cells expressing AKAR, a FRET-based PKA activity reporter, revealed single-cell PKA activity oscillations (n = 21). (C) Pseudocolor images of MIN6 β cells expressing AKAR show oscillatory PKA activity after TEA treatment. The distribution of AKAR is shown by the YFP fluorescence image. Scale bar = 10 μm.

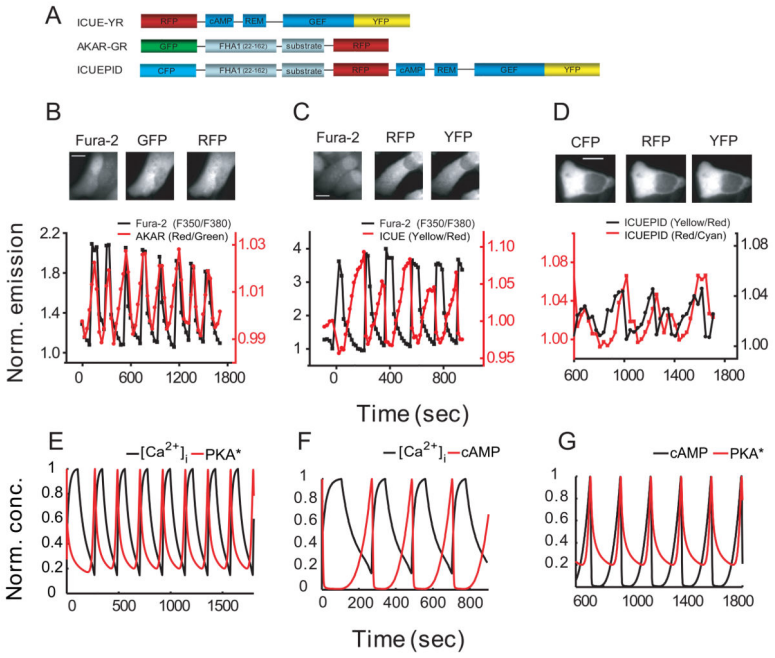

Figure 2.

Oscillatory changes in PKA activity, cAMP and Ca^{2+} dynamics are highly coordinated in MIN6 cells. (A) Domain structures of ICUE-YR, AKAR-GR, and a single-chain dual-specificity biosensor, ICUEPID, for PKA activity and cAMP dynamics. (B) (Top panel) Fluorescence images of MIN6 cells expressing AKAR-GR loaded with Fura-2. (Bottom Panel) Representative time courses showing coordinated oscillations in PKA activity (monitored by AKAR-GR, red) and Ca^{2+} (monitored by Fura-2, black) in single MIN6 cells. Scale bar = 10 μm. (C) (Top panel) Fluorescence images of a MIN6 cell expressing ICUE-YR loaded with Fura-2. (Bottom Panel) Representative time courses showing coordinated oscillations in cAMP (monitored by ICUE-YR, red) and Ca^{2+} (monitored by Fura-2, black) in single MIN6 cells. Scale bar = 10 μm. (D) (Top panel) Fluorescence images of a MIN6 cell expressing ICUEPID (bottom Panel). Representative time courses showing coordinated oscillations in PKA activity (red) and cAMP (black) monitored by ICUEPID in single MIN6 cells. Scale bar = 10 μm. (E) Simulation of the model showing Ca^{2+} (black) and active PKA (PKA*, red) oscillations. (F) Simulation of the mathematical model showing Ca^{2+} (black) and cAMP (red) oscillations. (G) Simulation of the model showing cAMP (black) and active PKA (PKA*, red) oscillations. Norm. emission and Norm. conc. refer to normalized emission and normalized concentration respectively, with normalization in simulations made with respect to the maximal value in the corresponding time course.

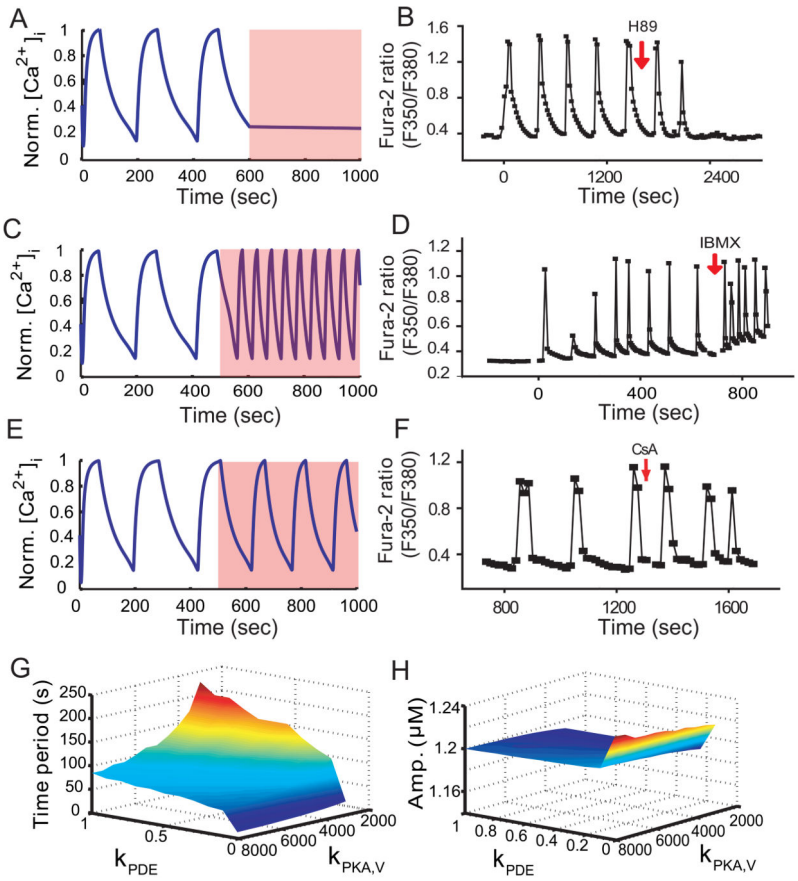

Figure 3.

PKA activity is required for Ca^{2+} oscillation and tunes its frequency. (A) Simulation of the model in the presence or absence of PKA (shaded region). (B) The effect of inhibiting PKA by H89 (10 μM) on Ca^{2+} oscillation. (C) Simulation of the model with increased feedback achieved when PDE activity is decreased (shaded region). (D) Effect of adding a PDE inhibitor IBMX (100 μM) on Ca^{2+} oscillations (n = 15). (E) Simulation of the model with increased feedback achieved when PP2B activity is decreased (shaded region). (F) Effect of adding a PP2B inhibitor cyclosporine A (CsA) (3 μM) on Ca^{2+} oscillations (n = 7). (G) Effect of PKA activation and activity parameters on the frequency of oscillations, simulated by the simultaneous variation of a parameter relating to the extent of PKA phosphorylation of channels ($k_{PKA,V}$) and a parameter controlling the maximal activity of PDE (k_{PDE}). (H) Effect of PKA activation and activity parameters on the amplitude of oscillations, simulated by the simultaneous variation of $k_{PKA,V}$ and k_{PDE}. Note the scale of the amplitude changes. Norm. $[Ca^{2+}]_i$ refers to intracellular Ca^{2+} concentration normalized to the maximal level and Amp. refers to amplitude of oscillations. See related analysis in the Supplementary Methods.

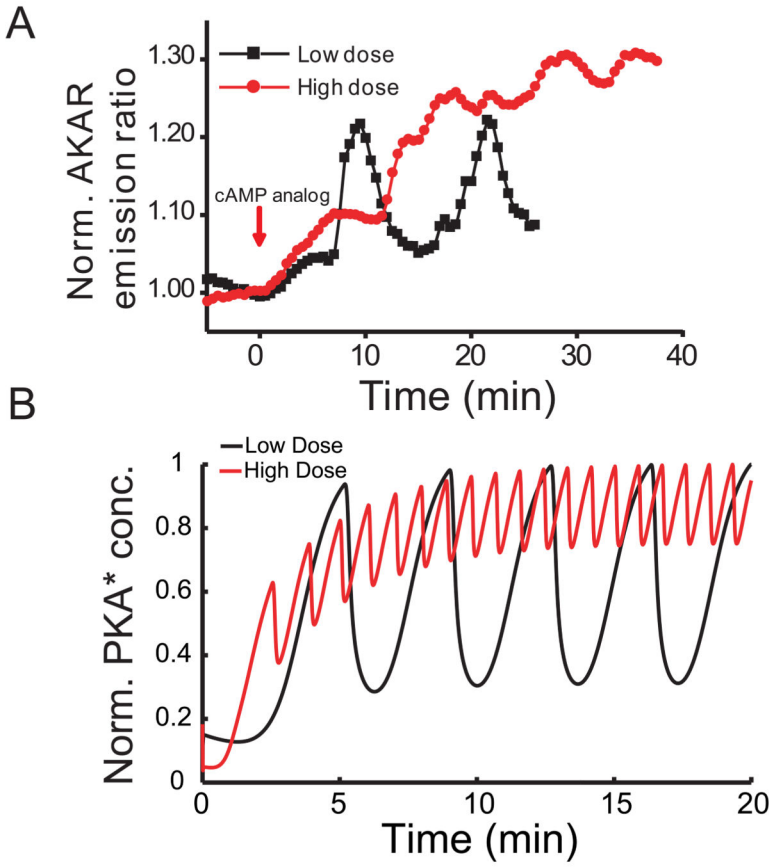

Figure 4.

Direct activation of PKA triggers the oscillation of the circuit. (A) Representative time courses showing oscillatory and sustained PKA behaviors upon stimulation with low (1–3 μM) and high (10–20 μM) doses of a PKA-specific cAMP analog, respectively (n = 16 and 13, respectively). (B) Simulation of the model showing the oscillatory and sustained PKA activities upon stimulation with low and high levels of cAMP analog, reflecting the time needed for the analog accumulation in the simulated cells.

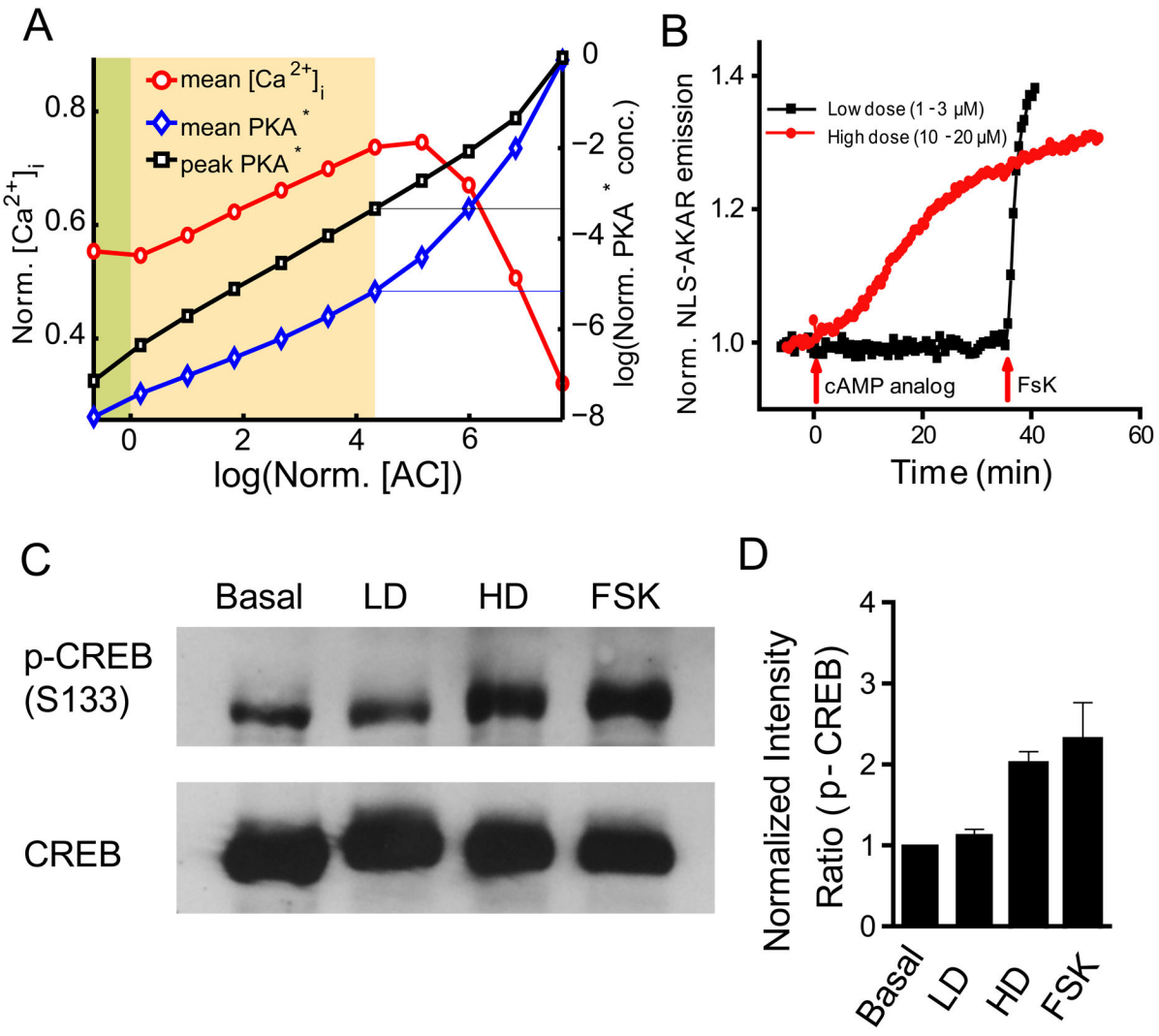

Figure 5.

Oscillatory PKA activity confers spatial control of substrates. (A) Simulation of the model showing the indirect activities of local (normalized mean [Ca^{2+}]) and global (using normalized mean PKA C-subunit concentration as a proxy) targets of PKA activation upon increase in the input AC activity and hence frequency of oscillations. The expected "local-activation" regime, defined by the AC activity at which the difference between log (Normalized mean PKAactivity) and log (Normalized peak PKAactivity) is maximal, is shaded in orange. The area shaded in green is bounded by the nominal AC activity, reflecting the expected physiological scenario. (B) Representative time courses of nuclear localized AKAR (NLS-AKAR) showing the absence and presence of nuclear PKA activity upon stimulation with low (1–3 μM) and high (10–20 μM) doses of a PKA-specific cAMP analog, respectively (n = 7 and 4, respectively). (C) Phospho-immunoblot analysis using antiphospho-CREB (pS133) shows no changes in CREB phosphorylation upon stimulation with a low dose (LD) of the cAMP analog (2 μM), while increased phosphorylation of CREB is observed upon stimulation with a high dose (HD) of the same cAMP analog (10 μM) or 50 μM forskolin (FSK). (D) Densitometric analysis of phosphorylated CREB

(pS133) (n =3) normalized to CREB expression shows a significant difference between the levels of CREB phosphorylation stimulated by the low and high doses of the cAMP analog.